International Journal of Engineering Trends and Technology
ISSN: 2231-5381/ https://doi.org/10.14445/22315381/IJETT-V73I3P113

Volume 73 Issue 3, 174-182, March 2025

Review Article

Thin Film Analysis by Infrared Spectroscopy

Ho Soonmin[1], Olasanmi Oluwatoyin O[2]

[1]*Faculty of Health and Life Sciences, INTI International University, Putra Nilai, 71800, Negeri Sembilan, Malaysia.*
[2]*Faculty of Physical Sciences, Department of Physics, University of Ilorin, Ilorin, Kwara State, Nigeria*.

[1]*Corresponding Author : soonmin.ho@newinti.edu.my*

Received: 13 August 2024 Revised: 21 November 2024 Accepted: 11 February 2025 Published: 28 March 2025

Abstract *- Metal chalcogenide thin films have been synthesized through various deposition techniques. These films have found numerous applications, including in solar cells, opto-electronic devices, laser systems, sensors, electroluminescent devices, and light-emitting diodes. A range of analytical tools has been employed for the characterization of these thin films, including X-ray diffraction, atomic force microscopy, scanning electron microscopy, energy dispersive X-ray analysis, UV-visible spectrophotometry, Raman spectroscopy, photoluminescence spectroscopy, and X-ray photoelectron spectroscopy. In this study, different types of thin films were produced using both physical and chemical deposition methods. The analytical method known as Fourier Transform Infrared Spectroscopy is used to identify organic, polymeric, and occasionally inorganic materials. Infrared light is used in the FTIR analysis method to scan test samples and observe chemical properties from 4000 cm^{-1} to 400 cm^{-1}. FTIR spectra indicated that the characteristic peaks were influenced by variations in experimental parameters such as temperature, heating processes, pH levels, and the presence of complexing agents, solution concentration, deposition duration, and the number of deposition cycles.*

Keywords *- Thin films, Solar cells, Energy efficiency, Energy consumption, Fourier transform infrared spectroscopy.*

1. Introduction

Thin films are layers of materials with thickness in the order of nanometer to several micrometres and have remained the basis for the development of numerous semiconductor devices [1]. In solar cell fabrication, thin film technology belongs to the second-generation class, an evolution from the first-generation technology based on crystalline silicon. Thin film solar cells employ multiple thin film layers of photovoltaic elements onto a substrate. It has received much attention recently because of its potential for substantial cost reduction advantage over traditional wafer-based crystalline silicon because of its lower material use and fewer processing steps. Thus far, Cadmium Telluride (CdTe), Copper Indium Gallium Selenide (CIGS), and Copper Zinc Tin Sulfide (CZTS) and Amorphous Silicon (a-Si) based thin film solar cells have been most widely commercialized. The common feature of these semiconductor materials is their direct band gap nature, which allows for the use of very thin material. So far, research on thin film technology based on CIGS, CdTe, and CZTS solar cells has recorded laboratory efficiency of 23.35%, 21.0%, and 10.0%, respectively [2]. Recently, numerous researchers have focused their studies on binary, ternary, and quaternary semiconductors. These materials have found applications in various fields, including solar cells, cathode ray tubes, sensors, laser devices, optoelectronic devices, light-emitting diodes, infrared windows [3], and biological applications. Thin film solar cells are less expensive to manufacture and set up than other solar cell varieties. Thin film cells weigh less than other solar cell types since they require less semiconductor materials. This solar cell can be designed to be semi-transparent, enabling light to filter through. The perfect band gap (approximately 1.5 eV) for a solar cell aligns with the energy of photons found in the solar spectrum. This enables the cell to effectively capture light and transform it into electricity. A strong absorption coefficient enables effective light absorption even in thin material layers. Thin films can be fabricated using a range of deposition techniques, such as chemical bath deposition, electrodeposition [4], thermal evaporation, spray pyrolysis [5], magnetron sputtering, metal-organic chemical vapor deposition, molecular beam epitaxy, sol-gel spin coating [6], pulsed laser deposition, successive ionic layer adsorption and reaction, and e-beam evaporation [7]. Numerous researchers have reported on the properties of thin films produced through these various methods [8]. X-ray diffraction has been employed to ascertain the structural characteristics of the films. Atomic force microscopy and scanning electron microscopy have been utilized to analyze the morphology of the samples. Energy dispersive X-ray analysis has been applied to examine the elemental composition of the materials. The optical properties of the films, including band gap and absorption behavior, have been investigated using UV-visible spectrophotometry. Raman spectroscopy has been employed to ascertain the chemical composition and structure of the samples [9]. Photoluminescence spectra have been analyzed

to explore the electronic structure and properties of the materials. X-ray photoelectron spectroscopy has been used to evaluate the elemental composition, chemical state, and electronic state of the element present [10]. Fourier transform infrared spectroscopy is a technique that utilizes Fourier transform mathematically to analyze the wavelengths that materials absorb. Infrared radiation passes through a sample in infrared spectroscopy. The sample takes in some of the infrared energy while some is transmitted. The spectrum obtained provides the sample with a molecular fingerprint by showing the absorption and transmission of the molecules. No two distinct molecular arrangements yield the same infrared spectrum, like fingerprints. Consequently, infrared spectroscopy is beneficial for numerous analyses. FTIR spectroscopy is founded on the principle that radiation interference between two beams produces an interferogram.

The latter represents a signal generated because of the change in path length between the two beams reflected off two mirrors. The two areas of distance and frequency can be converted into one another through mathematical techniques. The major components of FTIR are emphasized Table 1. The Michelson interferometer is the key distinction between an FTIR and an IR spectrometer. It is essential for the FTIR spectrometer to divide a single light beam into two, thereby establishing distinct paths for both beams. It then merges the two beams and directs them into the detector, where the variations in the intensity of these beams are assessed based on the difference in their paths. In FTIR spectroscopy, employing an interferometer presents numerous benefits, including significantly enhanced optical throughput thanks to a slit-less optical design, leading to an elevated signal-to-noise ratio. The capability to gather data across various wavelengths simultaneously without requiring scanning through a moving prism.

Enhanced wavenumber resolution by employing a laser source for precise digital signal sampling and increasing the movement distance of the mirror in the interferometer. Drawbacks of FTIR methods include the fact that the molecule needs to be reactive in the infrared spectrum. For absorption to be detected when exposed to IR radiation, at least one vibrational motion must alter the net dipole moment of the molecule. Minimal elemental information is given to many samples. The substance under examination needs to be clear in the relevant spectral range. Choosing materials for interfacial engineering is crucial because the functional groups of the interfacial material can engage with the solar cells. Effective interfacial materials possess various functional groups, yet there are typical effects that the primary functional groups provide. The carboxyl group consists of carbon, oxygen and hydrogen. It is an organic functional group where a carbon atom creates a double bond with one oxygen atom and a single bond with a hydroxyl group. The carboxyl group undergoes ionization by shedding a hydrogen atom from the OH group, which releases a free proton. The carboxyl group participates in Lewis's acid-base reaction with metal ions. Materials containing carboxyl groups as interfacial modifiers can achieve band alignment and defect motivation, while conductivity can be enhanced due to increased charge mobility. Moreover, the alkyl chain, the hydrophobic part of the molecule, contributes to strong water stability in the solar cells. An amine group refers to a functional group that consists of a nitrogen atom bonded to two hydrogens along with an alkyl or aromatic group. A material with an amine group at the interface can act as a Lewis base and provide a nitrogen lone electron pair to the empty orbital of the under-coordinated lead ions in the perovskite solar cells, thereby creating a coordination bond with the perovskite.

This bond coordination slows down the crystallization rate of perovskite, assisting in creating a uniform and dense perovskite film featuring the desired crystal growth orientation and high crystallinity. Like aromatic compounds, aromatic rings are hydrocarbon substances featuring a conjugated planar ring structure. Among these, the most common are benzene, phenyl, thiophene, imidazole, pyrrole, and pyridine. The free π electrons within the aromatic ring enhanced charge transfer, while the conjugated structure supplies electrons for passivating defects in the solar cells. Additionally, the hydrophobic properties of the aromatic ring hinder the ingress of moisture and oxygen from the devices. In this study, nanostructured thin films were synthesized using various deposition techniques, and Fourier Transform Infrared Spectroscopy (FTIR) was utilized to identify the functional groups within the samples. Also, the benefits and limitations of the FTIR method will be described.

2. Methodology

To locate research articles published in English related to Fourier transform infrared analysis of thin films, the authors performed a literature review in pertinent journals from 1997 to 2024. The databases explored included Google Scholar, Taylor & Francis, ACS, Scopus, Wiley Online Library, Science Direct, and MDPI. The terms used included "thin film solar cells", "Fourier transform infrared analysis", "binary films", "ternary films", and "quaternary films".

3. Literature Survey

3.1. FTIR Studies of Binary Thin Films

Fourier Transform Infrared Spectroscopy (FTIR) is recognized as a non-destructive analytical technique [11] that yields insights into the functional groups present in a sample. The radiation source generates infrared radiation that traverses the sample via the interferometer. Common examples of radiation sources include silicon carbide, tungsten halogen lamps, and mercury discharge lamps. The FTIR spectrometer employs an interferometer to modulate the wavelength emitted from a broadband infrared source [12], allowing for rapid signal measurement [13]. The detector quantifies the intensity of light that is either transmitted or reflected, depending on its wavelength. The resulting infrared spectrum

serves as a distinctive fingerprint for thin films, with absorption peaks corresponding to the vibrational frequencies of atomic bonds [14]. Researchers have noted that no two compounds produce identical infrared spectra, as each material represents a unique arrangement of atoms. This characteristic underpins the utility of infrared spectroscopy in qualitative analysis. The advantages and limitations of FTIR and Atomic Force Microscopy (AFM) technique are summarized in Table 1. FTIR is an affordable and sustainable technology for examining the characteristics of thin films. FTIR technique can quickly adapt to new demands and is a strong research resource.

Table 1. Advantages and limitations of the FTIR technique

Advantages	Limitations
FTIR	
Brightness	Cannot detect atoms [18]
Simple mechanical design [15]	Hard to analyse, especially in an aqueous solution
Universal technique	Cannot detect nitrogen and oxygen
Easy technique	complex spectra were produced [16]
Inexpensive technique	artifacts were produced
Internally calibrated	
Better sensitivity [17]	
All the frequencies could be recorded simultaneously.	
AFM	
achieve high-resolution images	scan a single image at a time
provide qualitative and quantitative information	images can contain artifacts

Tin oxide films have gained popularity as transparent conductors due to their excellent optical transparency in visible areas, mechanical stability, chemical corrosion resistance, and the raw materials' cost-effectiveness. These films possess a quadrangular structure and exhibit a band gap energy ranging from 3.7 to 4.2 eV. Ala and colleagues [18] have documented the production of high-purity SnO_2 films with a polycrystalline structure characterized by a tetragonal cassiterite phase. Examining the films through Field Emission Scanning Electron Microscopy (FESEM) images reveals they are free from cracks, exhibit uniformity, and possess a continuous grain distribution.

An FTIR analysis indicates two peaks at 613 cm^{-1} (Sn-O-Sn) and 3451 cm^{-1} (hydroxyl group), which are accountable for water (environmental humidity). Cadmium Sulfide (CdS) nanocrystalline displays three crystal structures: hexagonal quartzite, cubic zinc blend, and high-pressure rock-salt phase, demonstrating size-dependent properties. Its applications include serving as window material in heterojunction solar cells, being utilized as n-type material alongside p-type materials, and functioning in light-emitting diodes, photodetectors, field effect transistors, and electrically driven lasers. Hadeel and co-workers [19] have examined the optical and structural characteristics of CdS nanoparticles produced by the sol-gel technique with the surfactant Cetrimoniumm Bromide (CTAB).

The FTIR results demonstrated that the -OH group is responsible for a sizable absorption peak corresponding to 3450 cm^{-1} and represents the stretching vibration of the absorbed water on the CdS surface. The OH bending vibration of water molecules is responsible for the absorption band observed at 1635 cm^{-1}. The intense peak of the absorbed CO_2's C-O stretching vibration is located at 1033 cm^{-1}. The O-C=O asymmetric stretching vibrations are responsible for the absorption peak at 1394 cm^{-1}. The nanostructured CdS film [20] has been produced via a microemulsion-mediated sonochemical method.

Fourier Transform Infrared spectra reveal three prominent peaks at 635.54 cm^{-1} (indicating the stretching frequency of the CdS bond), 3429 cm^{-1} (corresponding to OH stretching), and 1629 cm^{-1} (representing the OH bending mode). A chemical deposition of 0.45 μm thick copper oxide films was achieved on glass substrates through 20-second microscope glass slides [21] immersion in solutions containing copper complex and 1 M Sodium Hydroxide (NaOH). While the copper solution was kept at an ambient temperature, the NaOH solution's temperature was raised to 70 °C. The films' as-deposited and 200 °C-annealed spectra exhibit a prominent band with a single transmittance minimum of around 627 and 619 cm^{-1}, respectively. The phonon spectrums of Cuprous Oxide (Cu_2O) and Cupric Oxide (CuO), which have wavenumbers of approximately 619 cm^{-1} and 532 cm^{-1}, respectively, are present in the films that have been annealed at 300 °C.

Broader peaks at around 535 cm^{-1} for the films that were annealed at 400 °C are similarly ascribed to the CuO stretching. It is also noted that for annealing temperatures above 300 °C, there is a clear peak at roughly 1120 cm^{-1}. After annealing at 300 °C, the FTIR spectroscopy observations verified that Cu_2O had transformed into CuO due to the disappearance of Cu_2O-associated peaks. Cadmium Selenide (CdSe) nanocrystals are employed in creating light-emitting diodes, solar cells, lasers, and other nanoscale devices, as well as helping comprehend the phenomenon of the quantum confinement effect. Many application studies have been conducted because of this material's blue shift in the band gap with decreasing grain size. Sodium selenosulphate is used as a Se^{2-} source during the chemical growth of CdSe (Eg = 1.7 eV), a direct band gap semiconductor [22]. Trisodium citrate, the capping agent utilized in this work, is confirmed to be present by the existence of the band at 1387 cm^{-1} and 1561 cm^{-1}, according to FTIR investigations. It is possible to attribute the latter band to the asymmetric COO^- and the former band

to the symmetric stretching of COO^-. Meanwhile, the band at 3368 cm^{-1} is attributed to OH stretching of trisodium citrate. Cadmium Selenide thin films were fabricated through a wet chemical synthesis approach [20]. The FTIR analysis identified several peaks at 624 cm^{-1} (stretching frequency of the CdSe bond), 3432 cm^{-1} (OH stretching), and 1628 cm^{-1} (OH bending mode). Because of its excellent optical and solid-state properties, Zinc Selenium (ZnSe), a group II-IV semiconductor compound, has attracted a lot of interest in the manufacture of solar energy devices.

It is a key component used in the creation of solar cells. It is a sort of direct band gap transition. ZnSe is a material of choice for visible transmission and low absorptiveness at infrared wavelengths, making it ideal for use in lenses, window layers, and output couplers.

Zinc Selenide thin films built on nanotechnology have a large direct band gap (3.87), good transmittance in the visible range, and are very desirable for use in optoelectronics and photonics applications. Using a chemical deposition approach, dye-sensitized ZnSe thin films were formed onto microscopic glass slides [23]. For sixty minutes, the films were placed at an even 80 °C. The presence of hydroxyl groups (O-H stretch, H-bonded) is indicated by a strong and broad peak obtained at 3235 cm^{-1}.

This observation may be related to the dye component phenol's easy ability to form intermolecular hydrogen bonds with water as well as the dye's easy electrophilic aromatic reaction with phenol, xanthophyll, and tannin. The C-H stretch is responsible for another prominent and wide spectrum peak located at 3390 cm^{-1}. Several contaminants were visible, including hydroxyl (O-H) and alkyne (C-H).

Hydroxyl groups could potentially. The chemical bath deposition of zinc selenide thin films was conducted under acidic conditions at a temperature of 80 °C, with varying deposition durations (60-240 minutes). FTIR analysis revealed peaks at 637 and 1148 cm^{-1} (stretching vibration), 877 cm^{-1} (C-H bending), 1412 cm^{-1} (bending vibration of CH_2), and 1587, 3261, and 3473 cm^{-1} (OH stretching mode) across all prepared samples [24].

Depending on its composition, zinc sulfide can have a large direct band gap (less than 3.5 eV), placing it in the II-VI group materials. Zinc sulfide, or ZnS, is a significant semiconducting material promising for optoelectronic devices like photovoltaic cells and electroluminescent devices due to its broad direct band gap and n-type conductivity.

ZnS thin films are made using the spray pyrolysis method. Basically, spray pyrolysis is a chemical deposition technique where a heated substrate is sprayed with fine droplets of the desired material solution. The optical characteristics and composition of the film structure are highly dependent on the deposition temperature, as observed by Djelloul and colleagues [25]. Films are amorphous when the deposition temperature is low. The films developed a stoichiometric ZnS composition and a polycrystalline (111) preferential orientation as the temperature increased. ZnS nanoparticle formation is confirmed by FTIR data. All samples exhibited weak, distinctive vibrations of zinc sulfide, which were found at 611 points 45 and 680 cm^{-1}. The formation of ZnS nanoparticles is responsible for the other peaks. ZnS films (spray pyrolysis method) exhibited a significant wide band gap of over 3.5 eV. FTIR analysis detected several weak vibrational peaks, specifically at 611.45 cm^{-1} and 680 cm^{-1} for films prepared at temperatures of 350 °C and 400 °C, respectively.

Zinc oxide absorbs and blocks harmful UV radiation. Its visible spectrum transparency allows it to penetrate the semiconductor layers underneath. Its chemical stability protects against environmental deterioration and ensures long-term durability. Its compatibility with thin-film deposition methods, such as casting and spraying, makes it a viable option for manufacturing processes as well. This enhances solar panels' overall performance and dependability when exposed to UV radiation.

Although manufacturers can add ZnO to adhesive, ZnO-based coatings can only be applied externally to solar panels that have already been installed. The right matrix and cost-effective deposition technique are needed for external ZnO-based coatings to be effective. When zinc oxide was employed for solar cell applications, some polymers such as polyvinyl butyral (encapsulant) and ethylene vinyl acetate (as layer) played an important role. PVB is well known for shielding surrounding elements by enclosing solar cells and blocking UV rays. To be more precise, PVB's primary duty in terms of protecting EVA is to assist in encasing and shielding the complete solar cell structure.

By keeping dust, moisture, and other external elements away from solar panels, PVB can prevent potential damage. As shown in Figure 1, several peaks could be found at 665-750 cm^{-1} and 1450-1500cm^{-1}, representing the C=C bond and the C-H bond, respectively. 3D transition metal impurities in semiconductor nanoparticles have attracted much attention recently due to their influence on emission band tuning. Analyzing commercially doped In_2S_3 will provide an alternative viewpoint for understanding the material's energy-related applications.

In addition to being less expensive, commercial In_2S_3 powder produces equally encouraging results compared to laboratory-made powder. Researchers conducted a thorough investigation into the properties of $In_{2-x}S_3Ni_x$ powders with 0, 2, 4, and 6 atomic proportions of nickel. FTIR data confirmed that all $In_{2-x}S_3Ni_x$ films were crystalline. All samples displayed semiconductor behavior, according to the impedance

analysis, and resistance dropped as Ni content rose.

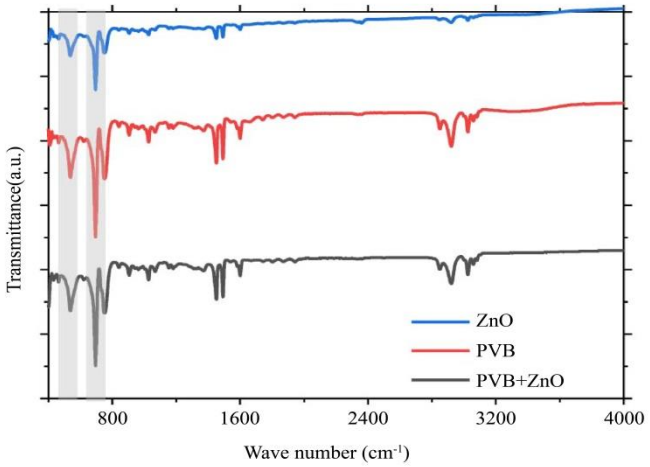

Fig. 1 FTIR of ZnO and PVB-ZnO samples [28]

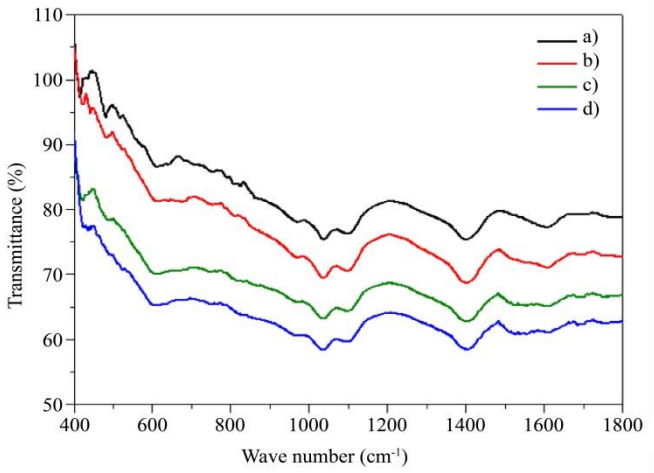

Fig. 2 FTIR spectra of different samples (a-In2S3, b-2% Ni-In2S3, c-4% Ni-In2S3, and d-6% Ni-In2S3) [29]

Information regarding the chemical composition of each sample was revealed by the FTIR spectral fingerprints in the 100–600 cm^{-1} wavenumber range [27]. Figure 2 shows three absorption bands, indicative of the stretching of C=O bonds and the O-H and C-H bond extensions at 1000–1500 cm^{-1}. With the rapid development of the photovoltaic industry, the aesthetic performance of solar modules is becoming more and more significant. One example of this is the development of integrated photovoltaic systems. Multi-crystalline silicon solar cells manufactured in industrial mass production usually have a layer of SiNx:H on the front surface, which is deposited using plasma-enhanced chemical vapor deposition. This layer acts as a passivation and antireflection layer. When the SiNx:H ratio is optimized for thickness and refractive index, the colors of solar cells appear light blue. Minghua [30], along with others, has focused on depositing a SiO_2 layer over the standard SiNx:H after the conventional mc-Si cell fabrication process using the electron beam (e-beam) evaporation technique and replacing the single SiNx:H layer with SiO_2/SiNx:H DARC. The band in the range of 1040-1150 cm^{-1} is identified as stretching vibration Si-O. A distinct Si-O intensity peak (1074 cm^{-1}) is observed for the oxygen supplement during the SiO_2 deposition.

3.2. FTIR Studies of Ternary Thin Films

$CuInSe_2$ has emerged as a top material for large-scale applications. It features excellent thermal stability, stability against photodegradation, a direct band gap, and a high absorption coefficient (>10^3 cm^{-1}). Its high absorption capacity allows it to absorb over 90% of the photon energy. One of the most inexpensive and promising materials for thin-film solar cells is $CuInSe_2$. As a result, these solar cells are among the best available for producing solar light, a renewable energy source. Using the electrodeposition method, $CuInSe_2$ thin films were created at pH 2.1, with deposition potentials of -500 or -600 mV in relation to a saturated calomel electrode and at different temperatures [29]. Several peaks were attributed to $CuInSe_2$ at 2345 cm^{-1} and $CuInSe_2$ at 3650 and 3844 cm^{-1} for the films prepared at 25 °C and -500 mV. Also, distinct absorption peaks at 2857 cm^{-1} and 3295 cm^{-1} (attributed to $CuInSe_2$) were observed (40 °C, -600 mV). Using the electrodeposition technique, ternary compounds, more precisely Cu-S-Se films, were created on fluorine-doped tin oxide glass substrates. All samples showed the presence of two distinct peaks at 1110 cm^{-1} (stretching vibration of CuSe) and 615 cm^{-1}, linked to the stretching vibration of CuS.

Peak intensity has been changed in response to the changes in selenium and sulfur ion composition, as shown by the FTIR spectra [30]. High-quality crystalline Cu_2SnSe_3 thin films have been shown to form on fluorine-doped tin oxide glass substrates. Strong peaks between 3300 and 2800 cm^{-1}, corresponding to C-H and N-H stretching vibrations, were seen in the as-deposited thin films. However, after being heated to 370 °C, the strength of these peaks decreased [31]. $CuInS_2$ has gained significant attention recently as a potentially useful material for the absorber layer in photovoltaic devices due to its high absorption coefficient (10^5 cm^{-1}), good stability for solar radiation, and direct band gap of approximately 1.5 eV, which falls within the ideal spectrum range for solar energy conversion. Additionally, n- and p-type solar cells can be produced by adjusting the $CuInS_2$ stoichiometric deviation, which is advantageous for both homojunction and heterojunction solar cells. Films rich in indium can form n-type $CuInS_2$, whereas films rich in copper can form p-type $CuInS_2$. Furthermore, because $CuInS_2$ does not contain any toxic elements like tellurium and selenium, it can be synthesized in an environmentally friendly environment. As a result, the environmental threat posed by chemical toxicity can be reduced. The electrodeposition method was used to synthesise copper indium disulfide thin films on fluorine-doped tin oxide glass at pH 12.5, with a sulfurization step that followed.

The deposition potential used was -0.75 V concerning Ag/AgCl. Several distinctive peaks were visible in the films made using Cu (Salen) complexes, including those at 1125 and 1192 cm^{-1} (phenolic CO bond), 736 cm^{-1} (phenyl group bonding mode = C-H), and 1630 cm^{-1} (C=N vibration). The films [32] synthesized with the presence of $Cu(acac)_2$ complexes showed clear, sharp peaks at 1415 cm^{-1} (C=C stretching mode), 782 cm^{-1} (phenyl group bonding mode = C-H), and a range from 454 to 616 cm^{-1} (CuO bond). Highly crystalline Cu_2SnS_3 films have been created using the chemical bath deposition technique on conductive stainless steel over the course of two hours at a pH of 4 [33]. Multiple peaks in the FTIR spectra indicated the presence of SnS at 1397 cm^{-1}, CuS and Cu_2S at 619 cm^{-1}, and SnS_2 in the sample.

Ethylenediamine tetraacetic acid disodium salt was used as a complexing agent to produce Cu_2SnS_3 films (substrate=fluorine-doped tin oxide glass substrates, 2 hours, 80 °C). Films prepared with different deposition times (60-90 minutes) were subjected to an FTIR analysis. Four distinct peaks were visible in the FTIR spectra at 619, 1122, 1397, and 1619 cm^{-1}. These peaks corresponded to the bending of OH in water, the vibration of the SnS bond, the asymmetric stretching of the carbonyl group, and the vibration of the Cu-S bond.

Furthermore, Sn-Sb-S films [34] were created on fluorine -doped tin oxide glass substrates using the spin coating technique. The pH values were created in the range of 1.56-1.80. The symmetrical stretching vibration mode of the O-C-O bond was found at 1607 cm^{-1}, the CO symmetric stretching vibration mode was found at 1400 to 1430 cm^{-1}, the SbS bond was found at 538 cm^{-1}, and the symmetric Sn-O-Sn was found at 455 cm^{-1}.

3.3. FTIR Studies of Quaternary Thin Films

Research has determined whether the kesterite compound Cu2ZnSnS4 (CZTS) qualifies as a non-toxic, less expensive, and earthly substitute for the binary and quaternary compounds. Because of their large absorption coefficient, over 104 cm−1, which results in lower material usage, and their direct optical bandgap in the range of 1.4-1.56 eV to exploit a greater magnitude of input solar irradiance from the spectrum, CZTS absorber layers are very promising materials. CZTS thin film is deposited using a new chemical SILAR technique.

Its foundation involves immersing the substrate one time at a time into distinct cation and anion precursor solutions, followed by rinsing with double distilled water to prevent precipitation in between. Ion-by-ion deposition causes the growth of thin films. In addition, surface coagulation of colloidal ions resulted in thin, adherent films. FTIR studies [35] show that a strong band at 3300 cm-1 appears connected to both symmetric and antisymmetric -N-H vibration modes. The NH2 bending, C=S stretching vibration, and NH2 rocking vibration deformation are attributed to the absorption peaks observed at 1645 cm-1, 1400 cm-1, and 1100 cm-1, respectively. Ahmad and colleagues [36] describe the synthesis and characterization of Cu2ZnSnS4 (CZTS) thin films made by the sol-gel method at various annealing temperatures and then immersed and deposited on glass substrates. In XRD analysis, tetrahedral kesterite could be observed when the anneal temperature was 450 °C.

FTIR analysis reveals that the sulfur-rich composition of the as-prepared CZTS films is responsible for their extended peak, which spans 3700 to 2500 cm-1. It was noted that the stretching and bending of oxygen are responsible for a sequence of peaks stretching from 900 to 1600 cm-1. The Zn–S and S–H bond stretching is visible in the peaks at 575 and 460 cm-1, respectively. The peak located at 1613 cm-1 may represent the symmetric stretching of the C-S bond. At 1062 cm-1 is the peak linked to the sulfur-rich Kesterite composition. The distinctive absorptions in 2070 and 2330 cm-1 are thiol group fingerprints.

Cu2ZnSnS4 (CZTS) films were synthesized using the hydrothermal method, as reported by Indubala and co-workers [37]. The films showed several distinct peaks after three hours of treatment at 650 °C. These peaks included 3433 cm-1, which indicates the presence of hydroxyl groups; 1638 cm-1, which is linked to the symmetrical stretching vibrations of the C-O bond; 1366 cm-1, which is related to the antisymmetric stretching vibrations of CO; 1123 cm-1, which is the C-O symmetric stretching frequency; and 616 cm-1, which is related to the ZnS band.

Copper zinc tin sulfide thin films with a direct band gap, multilayer structure, and high absorption coefficient make them appropriate for use in solar cell technology [38]. Equal amounts of zinc, tin, and copper were used to create the films, along with an excess of sulfur in a 1:3 ratio. The process was conducted for 180 minutes at different temperatures (350 to 650 °C). Indubala and co-workers have revealed five major peaks could be observed in these temperatures.

The metal ratios that were used had a big impact on the final CZTS film quality. The films were created under various reaction times and Cu: Sn ratios of 1.7 and 1.8 using acetonitrile as a solvent. FTIR analysis, however, revealed that there were no organic residues. At 320 °C, quaternary thin films, like Cu2ZnSnS4, were deposited on the specific substrate (soda lime glass) without the need for further sulfurization [39].

Distinct peaks were visible in the FTIR spectra at 630 cm-1 for ZnS, 1129 and 1651 cm-1 for metal thiourea complexes, 2369 and 2938 cm-1 for SH thiol, and 3460 cm-1 for thiourea. Olelamine (solvent and an electron donor) is selected in the hot injection method to prepare CZTS films [40]. FTIR studies highlighted the capping effect of oleylamine in

forming thin films. FTIR is an affordable and sustainable technology for examining the characteristics of thin films.

Table 2. Summary of disadvantages and advantages of FTIR, NMR and GPC

Technique	Disadvantages	Advantages
GPC	The GPC drench has a volume limit, and the effectiveness of chromatography depends on the volume of the macromolecular compound within a stated range.	Study the physico-chemical properties.
NMR	C-13: expensive analysis, a significant quantity of samples needed. H-1: no signals can be detected regarding internal carbon.	The peak positions of the NMR can indicate detailed information regarding the structure, chemical environment and functional groups of the samples
FTIR	Preparing samples is a tedious process. The accuracy resolution remains low.	Capability to show the category and substance of functional groups in the samples. A minimal sample size is needed.

The benefits and drawbacks of Nuclear Magnetic Resonance (NMR) and Gel Permeation Chromatography (GPC) techniques (Table 2) have been emphasized. FTIR technique can quickly adapt to new demands and is a strong research resource. Nuclear Magnetic Resonance (NMR) is a physical occurrence where nuclei within a strong uniform magnetic field are affected by a weak oscillating magnetic field and react by emitting an electromagnetic signal with a frequency specific to the magnetic field at the nucleus. This process occurs close to resonance, where the oscillation frequency aligns with the intrinsic frequency of the nuclei, influenced by the strength of the static magnetic field, the chemical surroundings, and the magnetic characteristics of the involved isotopes.

Gel Permeation Chromatography (GPC), referred to as Size Exclusion Chromatography (SEC), is a method employed to access the average molecular weight distribution of a polymer specimen. By utilizing the correct detectors and analytical methods, one can also acquire qualitative data on long-chain branching or ascertain the composition distribution of copolymers.

As suggested by its name, GPC or SEC classifies the polymer based on size or hydrodynamic radius. This is achieved by introducing a minimal quantity of polymer solution into a series of columns filled with porous beads. Smaller molecules can pass through the pores and are thus more than the larger molecules, which move down the columns and elute more quickly.

4. Conclusion

The thin film of metal chalcogenides has been produced using multiple deposition methods. These films have discovered various uses, such as solar panels, sensors, opto-electronic devices, laser technologies, sensors, electroluminescent gadgets and light-emitting diodes. A variety of analytical techniques have been used for the characterization of these films. In this research, Fourier Transform Infrared Spectroscopy (FTIR) was employed to recognize the presence of different types of functional groups in the obtained samples. FTIR analysis technique utilizes infrared light to examine samples from 400 to 4000 cm-1. FTIR spectra showed that the distinctive peaks were affected by changes in experimental parameters.

Funding Statement

The author (Ho SM) was financially supported by INTI International University, Malaysia.

Acknowledgments

This research work was financially supported by INTI International University, Malaysia (Ho SM).

References

[1] James A. Oke, and Tien-Chien Jen, "Atomic Layer Deposition and Other Thin Film Deposition Techniques: from Principles to Film Properties," *Journal of Materials Research and Technology*, vol. 21, pp. 2481-2514, 2022. [CrossRef] [Google Scholar] [Publisher Link]

[2] Martin Green et al., "Solar Cell Efficiency Tables (version 57)," *Progress in Photovoltaics*, vol. 29, no. 1, pp. 3-15, 2024. [CrossRef] [Google Scholar] [Publisher Link]

[3] Bo Peng et al., "Transparent AlON Ceramic Combined with VO_2 Thin Film for Infrared and Terahertz Smart Window," *Ceramics International*, vol. 44, no. 12, pp. 13674-13680, 2018. [CrossRef] [Google Scholar] [Publisher Link]

[4] Divya Boosagulla, Ramachandraiah Allikayala, and Sarada V. Bulusu, "In Situ Aluminum Doped Zinc Oxide Thin Films by Pulse Electrodeposition for the All-Electrodeposited Cadmium-Free Copper Indium Diselenide Solar Cells," *Thin Solid Films*, vol. 802, 2024. [CrossRef] [Google Scholar] [Publisher Link]

[5] Md. Hasnat Rabbi et al., "Growth of High Quality Polycrystalline InGaO Thin Films by Spray Pyrolysis for Coplanar Thin-Film

Transistors on Polyimide Substrate," *Journal of Alloys and Compounds*, vol. 1002, 2024. [CrossRef] [Google Scholar] [Publisher Link]
[6] Muthukumar Murugesan, and S.R. Meher, "TiO_2-ZnO Composite Thin Films Fabricated by Sol-Gel Spin Coating for Room Temperature Impedometric Acetone Sensing," *Sensors and Actuators A: Physical*, vol. 369, 2024. [CrossRef] [Google Scholar] [Publisher Link]
[7] Mini Yadav, and Ajay Shankar, "Impact of Deposition Rate on Structural, Morphological and Optical Properties of E-Beam Evaporated Chromium Thin Film," *Materials Today Proceedings*, 2024. [CrossRef] [Google Scholar] [Publisher Link]
[8] Ghazi Aman Nowsherwan et al., "Numerical Optimization and Performance Evaluation of ZnPC:PC70BM Based Dye-Sensitized Solar Cell," *Scientific Reports*, vol. 13, no. 1, pp. 1-16, 2023. [CrossRef] [Google Scholar] [Publisher Link]
[9] Fiza Mumtaz et al., "Raman Spectroscopy Study and Dielectric Anomalies in $Bi_{1-x}Eu_x$ AFM FeO_3 Thin Films," *Thin Solid Films*, vol. 789, 2024. [CrossRef] [Google Scholar] [Publisher Link]
[10] Yun Fang et al., "In Situ NAP-XPS Study of CO_2 and H_2O Adsorption on Cerium Oxide Thin Films," *Chemical Physics Letters*, vol. 794, 2022. [CrossRef] [Google Scholar] [Publisher Link]
[11] Andrei Victor Sandu et al., *Modern Technologies of Thin Films Deposition: Chemical Phosphatation*, 1st ed., Materials Research Forum LLC, Millersville, pp. 1-158, 2018. [Google Scholar] [Publisher Link]
[12] George Charalambous, *Analysis of Foods and Beverages: Modern Techniques*, 1st ed., Elsevier, pp. 1-672, 2012. [Google Scholar] [Publisher Link]
[13] James W. Robinson, Eileen M. Skelly Frame, and George M. Frame, *Undergraduate Instrumental Analysis*, 7th ed., CRC Press, Boca Raton, pp. 1-1264, 2004. [CrossRef] [Google Scholar] [Publisher Link]
[14] Peter Larkin, *Infrared and Raman Spectroscopy: Principles and Spectral Interpretation*, 2nd ed., Elsevier, 2017. [Google Scholar] [Publisher Link]
[15] Peter R. Griffiths, James A. De Haseth, and James D. Winefordner, *Fourier Transform Infrared Spectroscopy*, 1st ed., John Wiley & Sons, New Jersey, 2007. [Google Scholar] [Publisher Link]
[16] Brian C. Smith, *Fundamentals of Fourier Transform Infrared Spectroscopy*, CRC Press, 1-207, 1995. [Google Scholar] [Publisher Link]
[17] Da-Wen Sun, *Infrared Spectroscopy for Food Quality Analysis and Control*, 1st ed., Academic Press, pp. 1-448, 2009. [Google Scholar] [Publisher Link]
[18] Ala F. Ahmed et al., "Plasma Treatment Effect on SnO_2-GO Nano-Heterojunction: Fabrication, Characterization and Optoelectronic Applications," *Applied Physics A*, vol. 127, 2021. [CrossRef] [Google Scholar] [Publisher Link]
[19] Hadeel Salih Mahdi et al., "Microstructural and Optical Properties of Sol Gel Synthesized CdS Nano Particles using CTAB as a Surfactant," *AIP Conference Proceedings*, Bhubaneswar, Odisha, India, vol. 1832, no. 1, pp. 1-4, 2017. [CrossRef] [Google Scholar] [Publisher Link]
[20] Aurobinda Acharya, G.S. Roy, and Rajkishore Mishra, "Comparative Study of Performance of CDS, CDSE Thin Film, CDS-PTH, CDSE-PTH Nanocomposite Thin Films Using SEM EDXA (Scanning Electron Microscope) and FTIR (Fourier Transform Infrared Spectroscopy)," *Latin American Journal of Physics Education*, vol. 4, no. 3, pp. 603-609, 2010. [Google Scholar] [Publisher Link]
[21] Mohd Rafie Johan et al., "Annealing Effects on the Properties of Copper Oxide Thin Films Prepared by Chemical Deposition," *International Journal of Electrochemical Science*, vol. 6, no. 12, pp. 6094- 6104, 2011. [CrossRef] [Google Scholar] [Publisher Link]
[22] Charita Mehta et al., "Effect of Deposition Parameters on the Optical and Electrical Properties of Nanocrystalline CDSE," *Chalcogenide Letters*, vol. 4, no. 11, pp. 133-138, 2007. [Google Scholar] [Publisher Link]
[23] Nworie Ikechukwu Christian et al., "Phytochemical, Optical and FTIR Studies of ZnSe Thin Films for Solar Energy Applications," *IOSR Journal of Applied Physics*, vol. 14, no. 1, pp. 25-29, 2022. [Google Scholar] [Publisher Link]
[24] R. Khalfi et al., "Effect of Deposition Time on Structural and Optical Properties of ZnSe Thin Films Grown by CBD Method," *Optical Materials*, vol. 106, 2020. [CrossRef] [Google Scholar] [Publisher Link]
[25] A. Djelloul et al., "Properties Study of ZnS Thin Films Prepared by Spray Pyrolysis Method," *Journal of Nano and Electronic Physics*, vol. 7, no. 4, pp. 1-5, 2015. [Google Scholar] [Publisher Link]
[26] Abdul Ghaffar, Iftikhar Ahmed Channa, and Ali Dad Chandio, "Mitigating UV-Induced Degradation in Solar Panels through ZnO Nanocomposite Coatings," *Sustainability*, vol. 16, no. 15, pp. 1-16, 2024. [CrossRef] [Google Scholar] [Publisher Link]
[27] Abdelmajid Timoumi et al., "Physical and Dielectric Properties of Ni-Doped In_2S_3 Powders for Optical Windows in Thin Film Solar Cells," *Materials*, vol. 14, no. 19, pp. 1-11, 2021. [CrossRef] [Google Scholar] [Publisher Link]
[28] Minghua Li et al., "Realization of Colored Multicrystalline Silicon Solar Cells with SiO_2/SiNx:H Double Layer Antireflection Coatings," *International Journal of Photoenergy*, vol. 2013, no. 1, pp. 1-8, 2013. [CrossRef] [Google Scholar] [Publisher Link]
[29] Abd El Hady Kashyout et al., "One Step Electrochemical Deposition and Characterization of $CuInSe_2$ Thin Films," *Alexandria Engineering Journal*, vol. 53, no. 3, pp. 731-736, 2014. [CrossRef] [Google Scholar] [Publisher Link]
[30] M.A. Yewale et al., "Electrochemical Synthesis of CuS_xSe_{1-x} Thin Film for Super Capacitor Application," *Journal of Alloys and Compounds*, vol. 754, pp. 56-63, 2018. [CrossRef] [Google Scholar] [Publisher Link]
[31] Feng Liu et al., "Earth Abundant Cu_2SnSe_3 Thin Film Counter Electrode for High Efficiency Quantum Dot Sensitized Solar Cells," *Journal of Power Sources*, vol. 292, pp. 7-14, 2015. [CrossRef] [Google Scholar] [Publisher Link]

[32] Mahdiyeh Esmaeili-Zare, and Mohsen Behpour, "Influence of Deposition Parameters on Surface Morphology and Application of $CuInS_2$ Thin Films in Solar Cell and Photocatalytic," *International Journal of Hydrogen Energy*, vol. 45, no. 32, pp. 16169-16182, 2020. [CrossRef] [Google Scholar] [Publisher Link]

[33] Harshad D. Shelke et al., "Influence of Deposition Temperature on the Structural, Morphological, Optical and Photo Electrochemical Properties of CBD Deposited Cu_2SnS_3 Thin Films," *Journal of Alloys and Compounds*, vol. 831, 2020. [CrossRef] [Google Scholar] [Publisher Link]

[34] Warunee Kumrueng et al., "Effect of pH Treatment on the Structural and Optical Properties of $Sn_6Sb_{10}S_{21}$ Thin Films Facilely Synthesized Using a Spin Coating Method," *Optical Materials*, vol. 105, 2020. [CrossRef] [Google Scholar] [Publisher Link]

[35] C.D. Lokhande et al., "Photosensitive Cu_2ZnSnS_4 (CZTS) Thin Film Grown at Room Temperature by Novel Chemical Method," *Invertis Journal of Renewable Energy*, vol. 1, no. 3, pp. 142-149, 2011. [Google Scholar] [Publisher Link]

[36] Ahmad A. Ahmad et al., "Computational and Experimental Characterizations of Annealed Cu_2ZnSnS_4 Thin Films," *Heliyon*, vol. 8, no. 1, pp. 1-10, 2022. [CrossRef] [Google Scholar] [Publisher Link]

[37] E. Indubala et al., "Unusual Composition of CZTS: Elemental Sulfurization and Solution Method," *Materials Today: Proceedings*, vol. 8, pp. 393-401, 2019. [CrossRef] [Google Scholar] [Publisher Link]

[38] E. Indubala et al., "Secondary Phases and Temperature Effect on the Synthesis and Sulfurization of CZTS," *Solar Energy*, vol. 173, pp. 215-224, 2018. [CrossRef] [Google Scholar] [Publisher Link]

[39] M. Patel, A. Ray, and I. Mukhopadhyay, "Structural, Optical and Electrical Properties of Spray Deposited CZTS Thin Films under a Non-Equilibrium Growth Condition," *Journal of Physics D: Applied Physics*, vol. 45, no. 44, pp. 1-11, 2012. [CrossRef] [Google Scholar] [Publisher Link]

[40] C. Imla Mary et al., "Synthesis and Characterization of Amine Capped Cu_2ZnSnS_4 (CZTS) Nanoparticles (NPs) for Solar Cell Application," *Materials Today: Proceedings*, vol. 4, no. 14, pp. 12484-12490, 2017. [CrossRef] [Google Scholar] [Publisher Link]